ADVANCED MATERIALS
www.advmat.de

Cascade Downregulation of the HER Family by a Dual-Targeted Recombinant Protein–Drug Conjugate to Inhibit Tumor Growth and Metastasis

Yang Yuan, Sensen Zhou, Cheng Li, Xiaoke Zhang, Hui Mao, Weizhi Chen, and Xiqun Jiang**

Human epidermal growth factor receptor type 2 (HER2)-targeted therapy can significantly improve the outcome of patients with HER2 positive cancer. However, relapse after this treatment remains a great challenge in the clinic due to tumor resistance, in which the HER network induces constitutive signal transduction. In addition, integrin receptors in the tumor extracellular matrix can mitigate the therapeutic effect of inhibitors to the growth factors receptors and tyrosine kinases. Here, the development of a recombinant protein (RP-HI) and its drug conjugates (RPDC-HI) to target both HER2 and integrin is reported. When simultaneously blocking HER2 and integrin by RP-HI, functions of the HER family and their interactions with the integrin are disrupted by downregulated expressions of HER family members, leading to inhibition of several downstream signal pathways. In combination with targeted delivery of the anticancer agent, doxorubicin (DOX), RPDC-HI significantly improves the tumor inhibition efficacy to 97.5% in treating HER2-positive breast cancer, comparing to 34.3% for free DOX. RPDC-HI shows even better antitumor efficiency than a monoclonal antibody, trastuzumab, when treating larger tumors. The developed dual-targeted RPDC platform offers a new and promising strategy for treating HER2-positive patients with synergistic therapeutic effects against tumor resistance to the conventional HER2-targeted treatment.

1. Introduction

Breast cancer has the highest incidence in the world and often presents highly heterogeneous pathological and molecular characteristics.[1] Amplification of the epidermal growth factor receptor (HER) family, including epidermal growth factor receptor 1 (HER1, EGFR), 2 (HER2), 3 (HER3), and 4 (HER4), in breast cancers is associated with disease initiation, progression, metastasis and resistance to treatments.[2] Most notably, HER2 is overexpressed in about 20% of breast cancer patients which contributes to poor prognosis.[3] Indeed, the clinically approved HER2-targeted therapeutics, such as tyrosine kinase inhibitors,[4] monoclonal antibodies,[5] and antibody–drug conjugates (ADCs),[6] have led to the dramatic improvement in outcomes of patients with HER2-positive breast cancers. However, blockade of HER2 alone is not enough in some cases.[7] For example, HER2-targeting monoclonal antibody trastuzumab (Ttzm) has modest activity with objective response rate 23–35% in patients with HER2 positive metastatic breast cancer,[8] as other members of the HER family can initiate the alternative survival pathway, leading to resistance to HER2-targeted treatment.[9] Another evidence is that blocking EGFR/HER2 with lapatinib led to upregulated HER3 expression, suggesting that HER3 amplification plays a role in the compensation mechanisms of EGFR/HER2 blockade.[10] In addition, incomplete HER family blockade allows homodimer and heterodimer formation of members of the HER family and acquires resistance to treatment.[11] More recently, it is reported that 16–36% of patients with HER2-positive breast tumors have heterogeneous HER2 expression on cancer cells which is associated with poor therapy response to the targeted therapy with monoclonal antibodies Ttzm and ADC Ttzm emtansine, and becomes huge obstacle for effective treatment of HER2 positive breast cancers using HER2-specific agents.[12] Thus, development of therapeutics capable of simultaneously inhibiting and/or downregulating multiple members of the HER family may hold the potential to treat this subtype of HER2 specific breast cancer. Earlier effort in developing mixed antibodies or combining the antibody-based therapy with kinase inhibitors to simultaneously target HER family members[13] supports the approach of downregulating all members of the HER family, preferably with a single agent platform that can provide synergistic actions to multiple targets.

Y. Yuan, S. Zhou, C. Li, X. Zhang, W. Chen, X. Jiang
MOE Key Laboratory of High Performance Polymer Materials and Technology, and Department of Polymer Science & Engineering
College of Chemistry and Chemical Engineering
Nanjing University
Nanjing 210093, China
E-mail: chenwz@nju.edu.cn; jiangx@nju.edu.cn
H. Mao
Department of Radiology and Imaging Sciences
Emory University
Atlanta, GA 30322, USA
The ORCID identification number(s) for the author(s) of this article can be found under https://doi.org/10.1002/adma.202201558.

DOI: 10.1002/adma.202201558

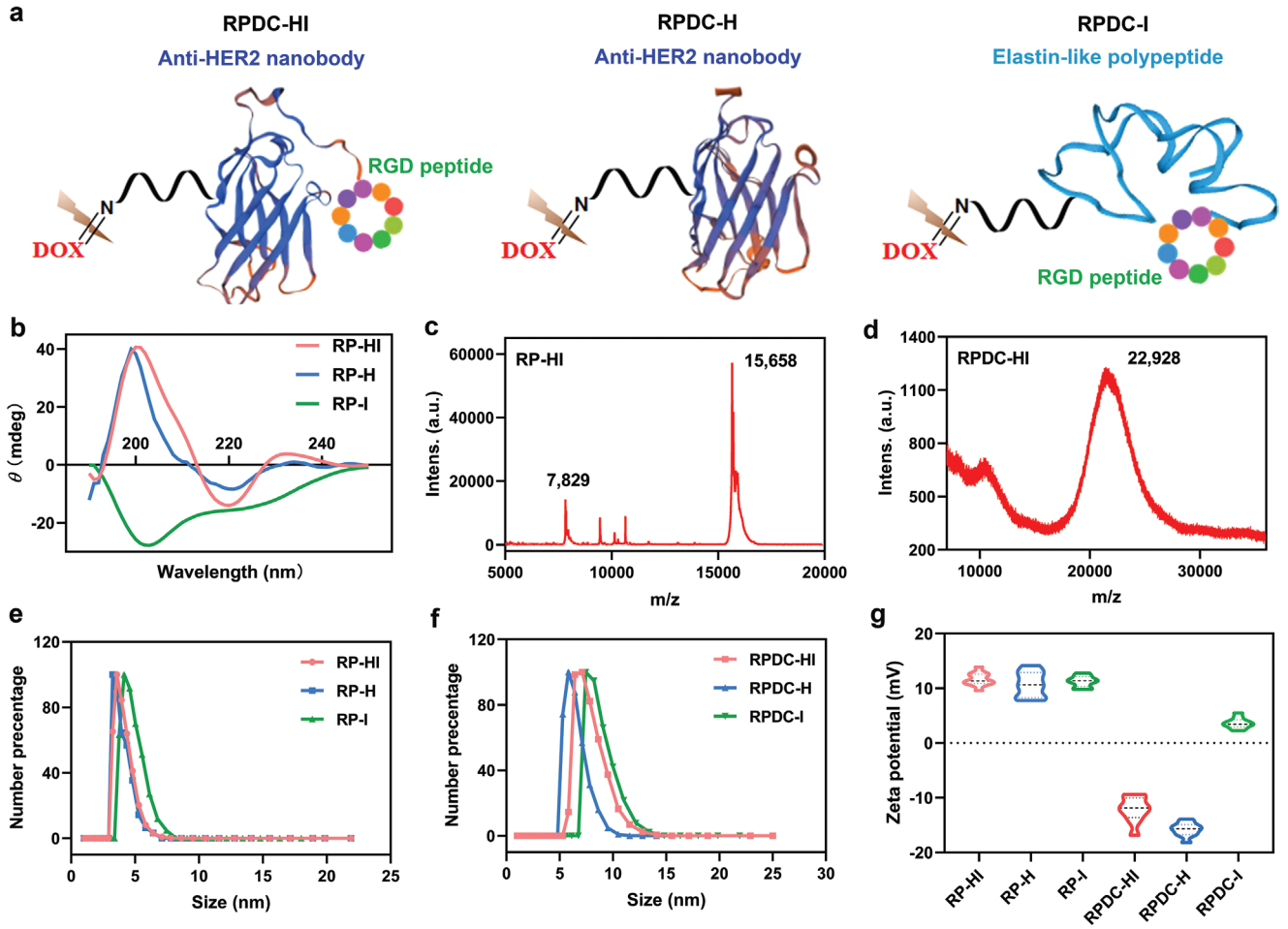

Figure 1. Design and preparations of RPDC-HI. a) Schematic illustration of three RPDCs, including HER2 and integrin $\alpha_v\beta_3$ dual-targeted RPDC-HI, HER2 single-targeted RPDC-H, and integrin $\alpha_v\beta_3$ single-targeted RPDC-I. b) CD spectrum of RP-HI, RP-H and RP-I. c,d) MALDI-TOF-MS analysis of RP-HI and RPDC-HI. e,f) The hydrodynamic sizes of RP-HI, RP-H, RP-I, and corresponding RPDCs determined by DLS analysis. g) Zeta potentials of three RPs and corresponding RPDCs ($n = 10$). Data are presented as mean ± standard deviation (SD).

Although members in the HER family playing key roles in the initiation of tumor cell proliferation are regulated by a wide range of ligands, such as growth factors and neuregulin,[14] malignancy development is facilitated by coordinated activities of HER family and other tumor associated regulators, including integrin.[15] For example, upregulation of integrin in the early-stage HER2-positive breast cancer patients is associated with the development of resistance to the HER2 and phosphoinositide 3-kinase (PI3K) combined therapy,[16] resulting the poor overall survival. Members of the HER family and integrin also promote metastasis in breast cancers.[17] Previous studies have demonstrated that signaling by HER family is closely coupled with signaling from the tumor integrin in regulating many cellular functions, such as cell adhesion, migration, and oncogenic transformation.[18] Amplification and activation of integrin signaling are also linked with the malignant features of breast cancer.[19] Thus, the interplay and cross-talk between HER family and integrin is a key regulatory process that involves in the development of drug resistance and metastasis in breast cancer.

Here we report a rationally designed recombinant protein–drug conjugate (RPDC-HI), which can simultaneously target both HER2 and integrin $\alpha_v\beta_3$ receptors. RPDC-HI consists of three key functional components, as shown in **Figure 1**a. The first component is a HER2 specific nanobody which has similar targeting ability to conventional HER2 monoclonal antibodies but with a smaller size. The second component is a cyclic RGD ligand (CRGDKGPDC) which can bind to integrin $\alpha_v\beta_3$ overexpressed in tumor cells. The third one is an anticancer agent, doxorubicin (DOX), covalently linked to HER2 specific nanobody through the pH-sensitive hydrazone bond and a polyethylene glycol oligomer spacer, which enables triggered drug release in the weak acidic tumor microenvironment. By disrupting HER2 in HER network functions and the interactions between the HER family and integrin, the dual-targeted RPDC-HI showed the capabilities of simultaneously downregulating all four HER family members, that is, EGFR, HER2, HER3, and HER4, at both gene and protein expression levels as well as blocking the downstream PI3K/protein kinase B (AKT) signaling pathways. These synergistic actions of RPDC-HI led to significantly superior therapeutic effect in reducing tumor size and inhibiting metastasis in the mouse model of HER2-positive breast cancer.

2. Results

2.1. Design and Preparations of RPDC-HI

The HER2 and integrin $\alpha_v\beta_3$ dual-targeted recombinant protein (RP-HI), HER2 single-targeted nanobody (RP-H), and integrin $\alpha_v\beta_3$ single-targeted RGD-integrated elastin polypeptide (RP-I) were expressed from *Escherichia coli (E. coli)*, respectively, as described in the Experimental Section in the Supporting Information. Their purities were first analyzed by sodium dodecyl sulfate polyacrylamide gel electrophoresis (Figure S1, Supporting Information) and a satisfactory purity of these recombinant proteins was obtained. Circular dichroism (CD) analysis showed that RP-HI and RP-H shared a similar β sheet conformation derived from the classic β-sheet structure of HER2 nanobody, while RP-I exhibited a random coil conformation (Figure 1b). Three RPDCs, that is, RPDC-HI, RPDC-H, and RPDC-I were then successfully obtained by covalently conjugating DOX to the RPs through a space linker made of bifunctional polyethylene glycol and an acid-labile hydrazone bond (Figure 1a). DOX is a clinical standard and generic anticancer drug used for treating many cancers in clinical oncology, including breast cancers.[20] More important, we found that the expressions of HER2 and integrin $\alpha_v\beta_3$ in MCF-7 cells increased after incubation with DOX (Figure S2, Supporting Information), suggesting that there is maybe a synergistic effect for the combination of RP-HI and DOX.

The molecular weights of RPs and the corresponding RPDCs were 15.7 and 22.9 kDa (RP-HI and RPDC-HI), 13.9 and 19.4 kDa (RP-H and RPDC-H), and 23.2 and 34.0 kDa (RP-I and RPDC-I) determined by matrix-assisted laser desorption ionization time-of-flight mass spectrometry (MALDI-TOF-MS) (Figure 1c,d and Figure S3, Supporting Information). On average, each RPDC carried 4 DOX molecules. Dynamic light scarring (DLS) analysis revealed that the hydrodynamic diameters of RP-HI, RP-H, and RP-I were around 3–5 nm (Figure 1e) and increased to 5–10 nm after conjugation of DOX (Figure 1f). The decrease of the zeta potentials from RPs (>11.3 mV) to the corresponding RPDCs (<3.6 mV) after the conjugation of DOX further confirmed the successful drug conjugation (Figure 1g). As the hydrazone bond was sensitive to low pH condition, these RPDCs exhibited a rapid DOX release behavior in acidic condition (Figure S4, Supporting Information).

2.2. HER2 and Integrin Dual Targeting and Targeted Cytotoxicity of RPDC-HI

The HER2 and integrin targeting capabilities of RPDC-HI, RPDC-H, and RPDC-I were first evaluated in vitro by confocal laser scanning microscopy (CLSM) and flow cytometry using human breast cancer MCF-7 cells which overexpress the receptors of the HER family and integrin $\alpha_v\beta_3$ (Figure S5, Supporting Information).[21] After incubation with MCF-7 cells for 2 h, HER2 and integrin $\alpha_v\beta_3$ dual-targeted RPDC-HI showed the highest intracellular DOX concentration among the three RPDC agents (**Figure 2**a–c). Quantitatively, the flow cytometry measured intracellular DOX fluorescence intensity in cells treated with RPDC-HI was 1.8- and 2.3-fold higher than those of RPDC-H and RPDC-I, respectively (Figure 2c). Further increasing incubation time with MCF-7 cells to 4 h, dual targeted RPDC-HI presented the highest intranuclear DOX concentration which was 1.8- and 1.6-fold higher than those of RPDC-H and RPDC-I, respectively (Figure 2d,e). Still, RPDC-HI maintained a highest intracellular DOX concentration (Figure 2f). After entering into MCF-7 cells, RPDC-HI was colocolated with lysosome, the acid microenvironment of which subsequently promoted DOX release from the RPDCs (Figure S6, Supporting Information), suggesting that simultaneously targeting both HER2 and integrin $\alpha_v\beta_3$ enhances the cellular uptake of RPDC-HI and subsequent DOX accumulation in both cytoplasm and nucleus.

In order to evaluate the effect of HER2 specific blockade to the cellular internalization of RPDCs, we pretreated MCF-7 cells with RP-H for 1 h to neutralize the HER2 receptors before incubation with RPDC-HI or RPDC-H for another 4 h. As a result, pretreatment with RP-H decreased the intracellular fluorescence intensity of RPDC-HI in treated cells by 30%, while signals from RPDC-H dropped by 60% (Figure 2g). Meanwhile, using RP-HI pretreatment also decreased the intracellular fluorescence intensity of RPDC-HI and RPDC-H in treated cells by 40% and 50%, respectively. This result confirms that there is a competitive cellular uptake between RP-HI and RPDC-HI or RP-H and RPDC-H. Next, we utilized monoclonal antibody Ttzm to neutralize the HER2 receptor. Interestingly, Ttzm pretreatment only decreased the intracellular fluorescence intensity of RPDC-HI and RPDC-H by 26% and 30%, respectively (Figure 2h). This result indicates that RP-H can largely inhibit cellular uptake of RPDC-H but not RPDC-HI, and has better cellular uptake inhibition effect than HER2-specific Ttzm on MCF-7 tumor cells, implying that RP-H may block more HER members than Ttzm. Endocytosis inhibition assay confirmed that the cellular entrance pathway of RPDC-HI and RPDC-H was clathrin-mediated endocytosis, while it was caveolae-mediated endocytosis for RPDC-I (Figure S7, Supporting Information).

Next, we evaluated the target specific cytotoxicity of RPs and RPDCs using the 3-(4,5-dimethylthiazol-2-yl)-2,5-diphenyltetrazolium bromide (MTT) assay. The half maximal inhibitory concentration (IC_{50}) values of RP-HI, RP-H and RP-I against MCF-7 cells were 680.3, 1015, and 938.5 μg mL^{-1}, respectively (Figure 2i and Figure S8a, Supporting Information), suggesting that HER2 and integrin $\alpha_v\beta_3$ dual-targeted RP-HI has a higher efficacy against the cells proliferation. For normal human mammary epithelial cell line, MCF-10A cells and human embryonic kidney HEK 293 cells, the RP-HI, RP-H and RP-I showed great cytocompatibility with cell viability over 80% after incubation with these RPs for 24 h even at the highest concentration (800 μg mL^{-1}) (Figure S8b,c, Supporting Information). In contrast, the IC_{50} values of RPDC-HI against MCF-7 cells was 5.03 μg mL^{-1}, much lower than that of RPDC-H (13.02 μg mL^{-1}) and RPDC-I (12.15 μg mL^{-1}), indicating that dual blockade of HER2 and integrin $\alpha_v\beta_3$ largely enhances the cytotoxicity of RPDC-HI compared to single targeted RPDCs (Figure 2i and Figure S8d, Supporting Information). This is consistent with that the dual-targeted RPDC-HI has a significantly enhanced ability in cellular internalization. Notably, IC_{50} value of free DOX was 1.97 μg mL^{-1}, consistent with the previous reports,[22] which was slightly lower than that of RPDC-HI.

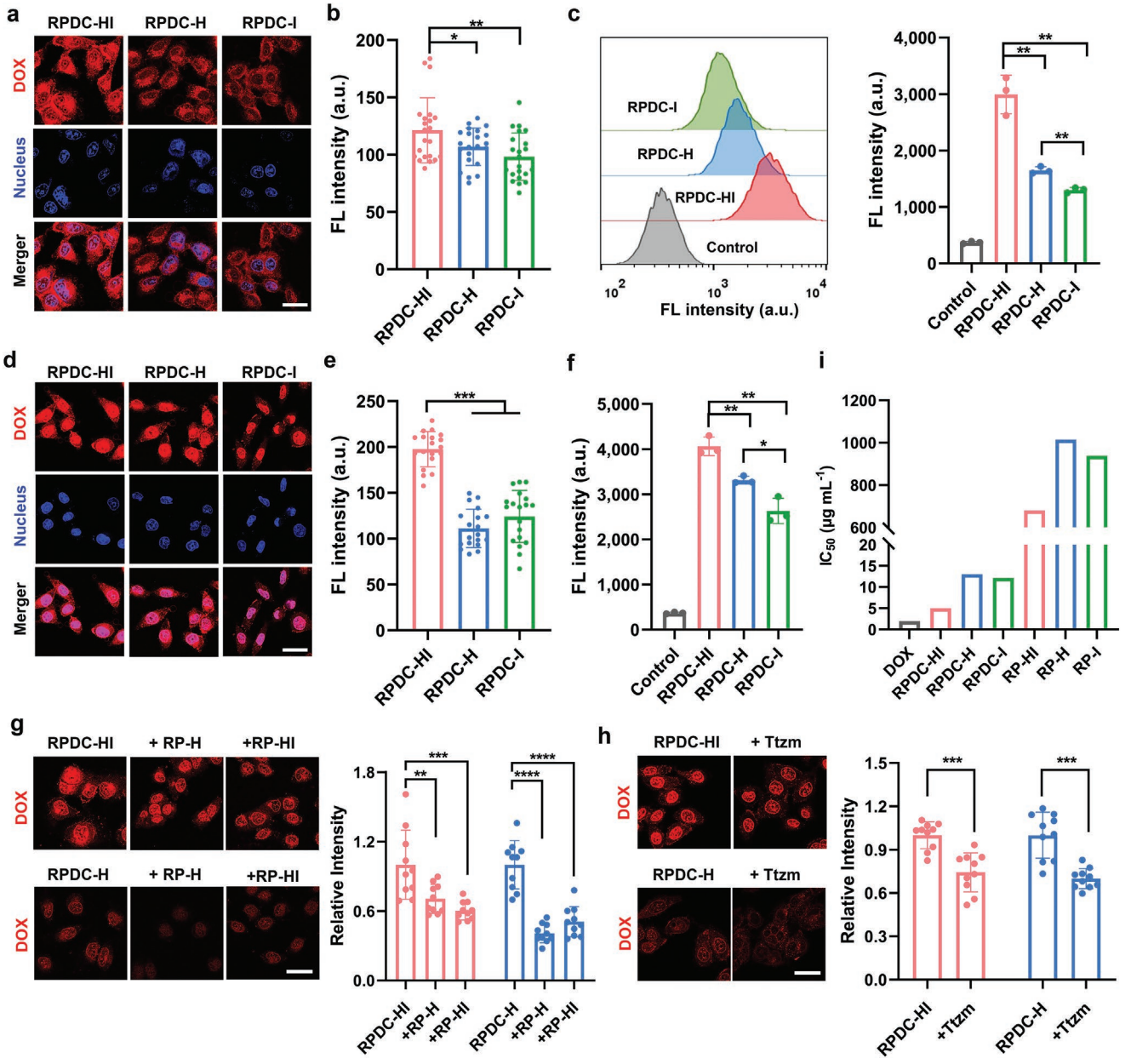

Figure 2. HER2 and integrin dual targeting and targeted cytotoxicity of RPDC-HI. a–c) Three kinds of RPDCs were incubated with MCF-7 cells for 2 h. The intracellular DOX distributions and intensity were then determined by CLSM (a) and flow cytometry (c). The fluorescence intensity of DOX in the nuclei of three RPDCs is shown in (b), ($n = 22$ for (b), 3 for (c)). d–f) Drug release from RPDCs in MCF-7 cells was time-dependent. The cellular internalization of RPDCs in MCF-7 cells after incubation for 4 h were further evaluated by CLSM (d) and flow cytometry (f); The fluorescence intensity of DOX in the nuclei of three RPDCs is shown in (e), ($n = 19$ for (e), 3 for (f)). g,h) CLSM images and the semiquantitative analysis of the fluorescence intensity of DOX in MCF-7 cells after incubation with RPDC-HI and RPDC-H, with or without RP-H, RP-HI (g) or Ttzm pretreatment (h), ($n = 10$ for (g) and (h)). i) The IC_{50} values of DOX, RPs, and RPDCs on MCF-7 cells were determined by MTT assay. Scale bar = 50 μm. Data are presented as mean ± SD, statistical significances were calculated using unpaired *t*-test, $^{*}p < 0.05$, $^{**}p < 0.01$, $^{***}p < 0.001$, $^{****}p < 0.0001$.

2.3. Diffusion and Distribution of RPDC-HI in Tumor Organoid and Excised Tumors

To investigate the intratumoral distribution of RPDCs, we used MCF-7 cells derived organoid to mimic the tumor for measuring the uptake and diffusion of RPDCs in vitro. A time-dependent increase of DOX fluorescence intensity in the MCF-7 organoid for all the RPDCs was observed (**Figure 3**a–d and Figure S9, Supporting Information). Analyzing the results from the measurement of the effective diffusion of RPDCs using fluorescence intensity over 60 a.u. from the periphery to the center of organoid as a threshold showed that diffusion distances of RPDC-HI, RPDC-H, and RPDC-I after 12 h incubation were 32, 32, and 22 μm, respectively (Figure S9a–c, Supporting Information). However, the diffusion distance of RPDC-HI became over 250 μm after 24 h incubation, much farther than 115 and 60 μm

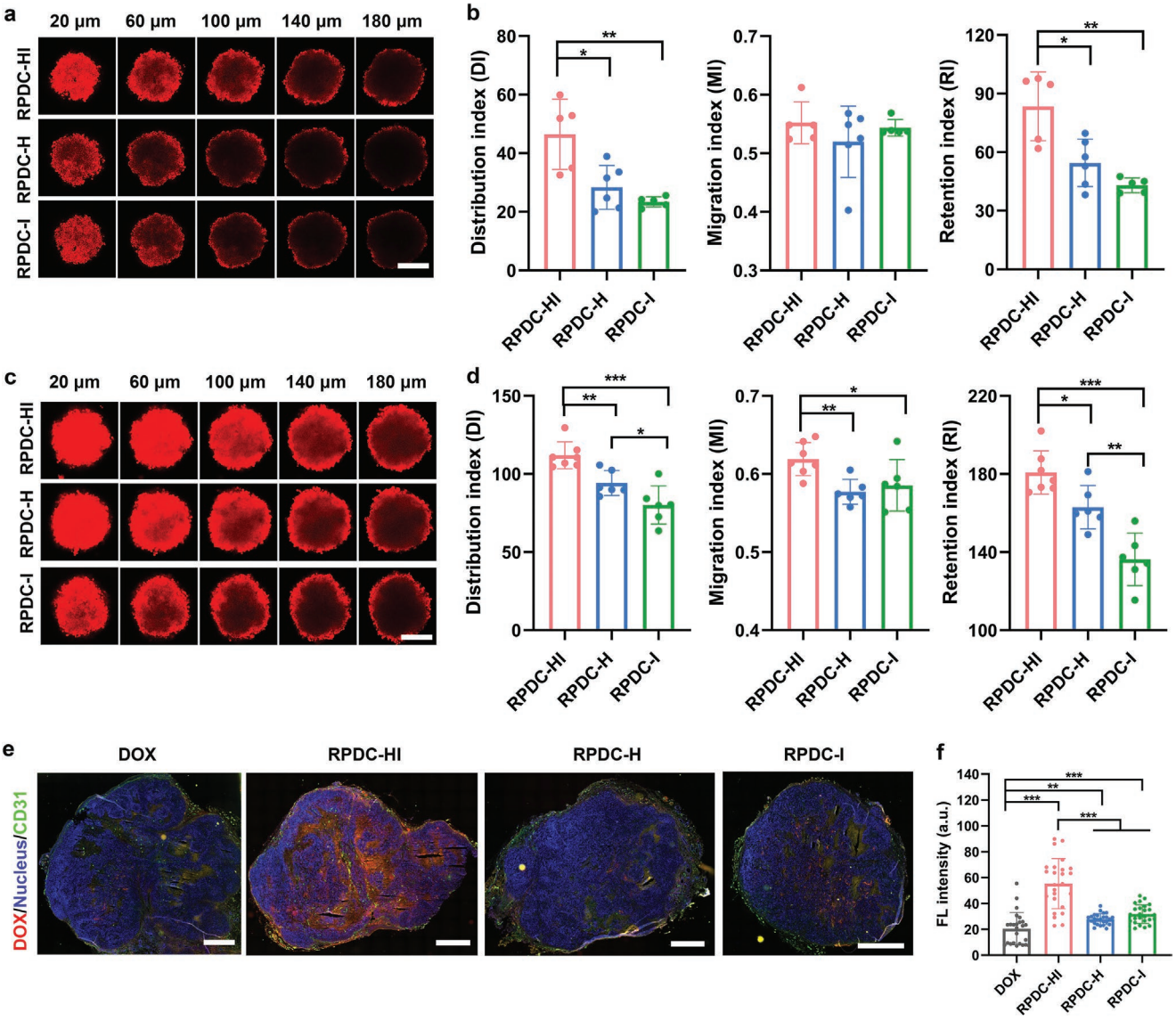

Figure 3. Diffusion and distribution of RPDC-HI in organoids and excised tumors. a–d) RPDC-HI improved drug distribution in organoids. a,c) The CLSM images of MCF-7 cells derived organoids after incubation with RPDCs for 12 h (a) and 24 h (c). Scale bar = 200 μm. b,d) The RI, DI, and MI of three RPDCs in MCF-7 cells derived organoids after incubation for 12 h (b) and 24 h (d) (n = 5–7). Data are presented as mean ± SD; statistical significances were calculated using unpaired t-test, $^{*}p < 0.05$, $^{**}p < 0.01$, $^{***}p < 0.001$. e,f) RPDC-HI showed an improved drug distribution in orthotopic xenograft MCF-7 tumors. DOX accumulation and distribution of free DOX and three RPDCs in the whole MCF-7 excised tumors observed by CLSM images (e), and further quantitatively analyzed by the DOX fluorescence intensity in avascular regions (f) (n = 25); scale bar = 1 mm. Data are presented as mean ± SD; statistical significances were calculated using multiple t-tests, $^{*}p < 0.05$, $^{**}p < 0.01$, $^{***}p < 0.001$.

observed from RPDC-H and RPDC-I (Figure S9d–f, Supporting Information). Quantitatively, we used distribution index (DI), retention index (RI), and migration index (MI) to evaluate the distribution, retention, and diffusion abilities of RPDCs.[23] RPDC-HI had the highest DI and RI compared to RPDC-H and RPDC-I after both 12 and 24 h incubation, although MI of RPDC-HI was similar to that of RPDC-H and RPDC-I at 12 h due to similar size (Figure 3b,d), suggesting that dual targeting of HER2 and integrin $\alpha_v\beta_3$ significantly improved the distribution and retention of RPDC-HI in the MCF-7 cell-derived organoid with a higher amount of drug accumulation and more homogenous drug distribution in the organoid.

Similar experiments were then repeated using excised tumor tissue collected from MCF-7 tumor-bearing mice after intravenously injection of three RPDCs to examine the intratumoral RPDCs distribution. Wide-field confocal microscopy analysis of the whole tumor in the range of 5–6 mm showed that RPDC-HI exhibited the most homogeneous intratumor distribution among all the RPDCs at 12 h post injection while free DOX was the least (Figure 3e). Analyzing fluorescence intensities of RPDCs in the avascular regions of whole tumor slices, we found that the value of RPDC-HI is 2.7-, 2-, and 1.7-fold higher than that of free DOX, RPDC-H, and RPDC-I (Figure 3f), which is consistent with the results obtained from the experiments

using MCF-7 cell derived organoid. In both sets of experiments, we observed improved diffusion and distribution by the HER2 and integrin $\alpha_v\beta_3$ dual targeting over single targeting.

2.4. Biodistribution and Tolerance of RPDC-HI

The pharmacokinetics of free DOX and RPDCs were evaluated using ICR mice. The plasma concentrations of DOX were measured after injection of free DOX or different RPDCs with an injection dosage (ID) of 5 mg kg^{-1}(DOX eq.). While DOX was undetectable at 15 min post injection for free DOX (**Figure 4**a), the measured half-life time of RPDC-HI, RPDC-H, and RPDC-I was 10.1, 4.5, and 11.5 h (noncompartment model),[23] respectively, suggesting that RPDCs significantly prolong the circulation time of DOX. To further evaluate the effects of dual targeting on the tumor specific uptake and accumulation, biodistribution of free DOX and RPDCs were investigated in BALB/C nude mice bearing orthotopic xenograft tumors growing from MCF-7 cells using an ID of 5 mg kg^{-1} (DOX eq.). The maximal tumor accumulation of RPDC-HI was measured at 6.8 ± 2.3% ID per gram of tissue (ID g^{-1}) at 12 h post injection, which was 12.6-, 2.1-, and 1.6-fold of those obtained from free DOX, RPDC-H, and RPDC-I, respectively (Figure 4b). At 24 h after injection, the intratumoral DOX content in the animals injected with free DOX was hardly measurable, while the intratumoral DOX content of RPDC-HI was about 5.1 ± 1.5% ID g^{-1}, which was 1.9 times of RPDC-H and RPDC-I, suggesting that a higher tumor accumulation and a longer tumor retention time as the result of HER2 and integrin $\alpha_v\beta_3$ dual

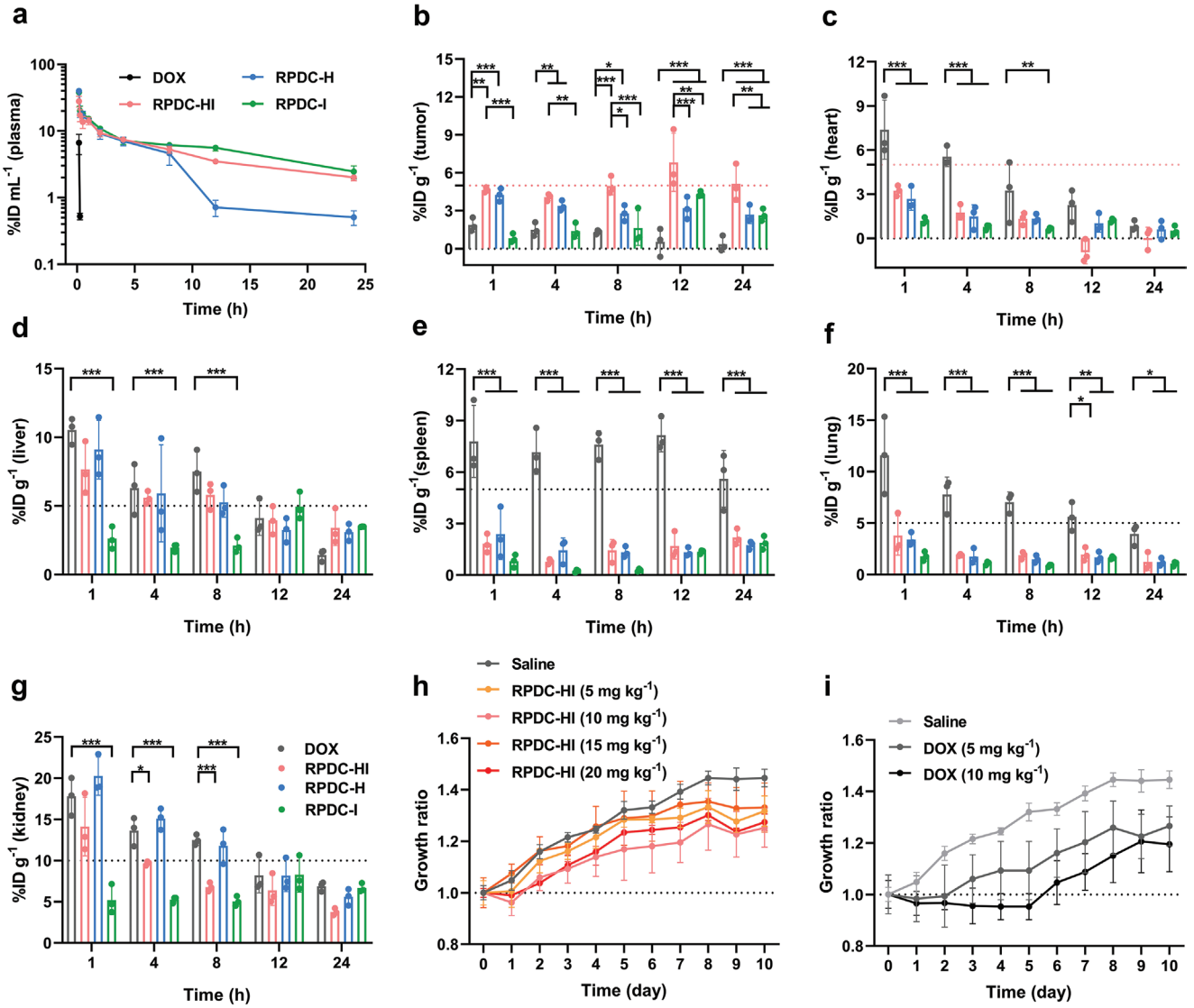

Figure 4. Biodistribution and tolerance of RPDC-HI. a) The pharmacokinetics of DOX, RPDC-HI, RPDC-H, and RPDC-I measured in ICR mice ($n = 3$). b–g) The drug accumulations of free DOX and three RPDCs in tumor (b), heart (c), liver (d), spleen (e), lung (f), and kidney (g) in the mice bearing orthotopic xenograft MCF-7 tumors at different time points post drug injection ($n = 3$). h,i) The body weight changes of ICR mice treated with different dosage of RPDC-HI (h) and free DOX (i) ($n = 2$ for RPDC-HI (20 mg kg^{-1}) group, $n = 3$ for others). Data are presented as mean ± SD, statistical significances were calculated using multiple *t*-tests, $^*p < 0.05$, $^{**}p < 0.01$, $^{***}p < 0.001$.

targeting by RPDC-HI. Worth noting, single targeted RPDC-H and RPDC-I also improved the intratumoral accumulation of DOX but at a lower degree than RPDC-HI. As far as the concern of cardiotoxicity associated with DOX largely limiting the chemotherapeutic applications of DOX, the averaged maximal concentration of DOX in heart at 1 h after injection (5 mg kg^{-1}, DOX eq.) was only 3.2 ± 0.5% for RPDC-HI compared with 7.4 ± 2.0% ID g^{-1} for free DOX-treated group (Figure 4c). In addition, DOX contents in liver, spleen, lung, and kidney were reduced in RPDC-HI group comparing to free DOX (Figure 4d–g). In all, RPDCs not only increase DOX accumulation at tumor sites but also reduce the DOX contents in healthy organs, with RPDC-HI representing the most efficient tumor specific accumulation.

Given the reduced accumulation of RPDCs in normal organs as shown above, the maximum tolerated dose (MTD) of RPDCs were then evaluated. The body weights of the mice treated with different dosages of free DOX and RPDCs were monitored daily for 10 days (Figure 4h,i and Figure S10, Supporting Information). The MTDs of RPDC-HI, RPDC-H, and RPDC-I were determined to be 20, 15, and 15 mg kg^{-1}, respectively, which were four, three, and three times higher than that of free DOX (5 mg kg^{-1}). To further confirm the biosafety of RPDCs, the plasma and organs from the mice treated with different agents at the respective MTDs were collected at day 10 post injection for serum biochemical test and H&E analysis (Figures S11 and S12, Supporting Information). No obvious injury to major organs was observed at RPDCs group.

2.5. Antitumor Efficiency of RPDC-HI

We next investigated the antitumor efficacy of RPDCs in the mouse model of HER2-positive breast cancer using the tumor volume and weight as measurements. Mice bearing orthotopic xenograft MCF-7 tumors were treated with free DOX and different RPDCs at the dosage of 5 mg kg^{-1}, DOX eq. (**Figure 5**a). As shown in Figure 5b,c, RPDC-HI exhibited the highest anticancer activity among the three RPDCs and free DOX. The significant tumor volume reduction, not just inhibition of the tumor growth, was observed in mice treated with RPDC-HI. Although the animals received RPDC-H showed a tumor volume reduction at initial days after first administration, the growth of tumors continued after a few days of the treatment. At day 18 after the first treatment, tumors grew to 5.62-, 3.46-, 0.80-, 1.76-, and 3.39-fold of their initial size in the groups treated with saline, free DOX, RPDC-HI, RPDC-H, and RPDC-I (Figure 5d). Only RPDC-HI showed a tumor volume reduction effect. The tumor sizes in RPDC-HI group were the smallest and the average tumor weight was 13.2 ± 4.9 mg, which was 7.5%, 18.0%, 39.5%, and 30.5% of that in the group of saline (176.7 ± 11.1 mg), free DOX (73.5 ± 31.7 mg), RPDC-H (33.4 ± 3.6 mg), and RPDC-I (43.2 ± 20.8 mg), respectively (Figure 5e). RPDC-HI displayed the best antitumor efficacy with negligible side effects (Figure S13a–c, Supporting Information).

Considering the MTD of RPDC-HI was four times higher than free DOX, the administered dosage of RPDC-HI was elevated to 10 mg kg^{-1}, DOX eq., a half of the MTD, for further evaluation of the antitumor effect. Compared to the low dose (5 mg kg^{-1}, DOX eq.), tumors treated with RPDC-HI (10 mg kg^{-1}, DOX eq.) exhibited continuous and more significant volume reduction (Figure 5f,g). The trend of tumor volume reduction was observed during the whole treatment period. The tumor volume at day 18 post first injection for RPDC-HI group was only 0.16 times of that measured at day 0 (Figure 5h and Figure S13d, Supporting Information). The tumor inhibition rate of RPDC-HI and free DOX were 97.5% and 34.3%, respectively. The average tumor weight for RPDC-HI group was 6.6 ± 2.5 mg at day 18 while this value was 76.9 ± 20.6 mg for free DOX and 119.0 ± 6.0 mg for the saline treated group (Figure 5i). Visually, RPDC-HI (10 mg kg^{-1}, DOX eq.) treatment achieved encouraging antitumor efficacy with negligible side effects (Figure S13e–g, Supporting Information). The exhibited better anticancer effect from HER2 and integrin $\alpha_v\beta_3$ dual-targeted RPDC-HI at both low and high dosage is likely attributed to the targeting toward HER network and integrin $\alpha_v\beta_3$ as well as enhanced intratumoral diffusion ability.

To approach the clinical test condition, the MCF-7 tumors with an average volume about 100 mm^3 were established to further evaluate the anticancer effect of RPDC-HI. In this case, Ttzm, the first-line monoclonal antibody treatment for breast cancer was used as positive control (Figure 5j). The ID of RPDC-HI was selected to be 10 mg kg^{-1} (DOX eq.), while ID of Ttzm was 4 mg kg^{-1}, a common dosage for Ttzm used in antitumor test.[24] As a result, RPDC-HI still made tumor to shrink at initial days after first administration even for the animal model with larger tumor volume (Figure 5j). The tumor grew up to 1.73-fold of initial size at day 18. In contrast, the tumors in Ttzm-treated group grew up to 6.28-fold, a similar rate to that of the saline-treated group (Figure S13h,i, Supporting Information). The tumor inhibition rate of RPDC-HI was 75% at day 18, while Ttzm could not efficiently inhibit the tumor growth and tumor inhibition rate was only 8.5% (Figure 5j), which maybe because the upregulation of EGFR and HER3 resisted HER2-targeted therapy of Ttzm (Figure S14, Supporting Information). Thus, the treatment with RPDC-HI inhibited the growth of larger tumors significantly. Importantly, RPDC-HI significantly improved the overall survival over Ttzm (Figure 5k). The median survival time for the groups receiving saline and Ttzm was 39 days, while it was beyond 55 days for the group of RPDC-HI, confirming the therapeutic potential of HER2 and integrin $\alpha_v\beta_3$ dual inhibition in breast cancer.

2.6. Inhibition of Metastasis by Dual-Targeted RPDC-HI

To investigate the effect of antimetastasis by RPDC-HI, the mice intravenously injected with 1×10^6 MCF-7 cells were subsequently treated with saline, free DOX, and RPDC-HI at day 0 and day 7 after cancer cells injection, while mice treated with saline were used as positive control and healthy mice were used as the negative control (**Figure 6**a). In this cancer metastasis model, distinct metastatic lesions were found in the livers and lungs of the mice treated with saline at day 70 after cancer cells injection (Figure 6b), suggesting that the metastatic model was established successfully. The average number of liver metastatic lesions in mice treated with saline, free DOX, and RPDC-HI

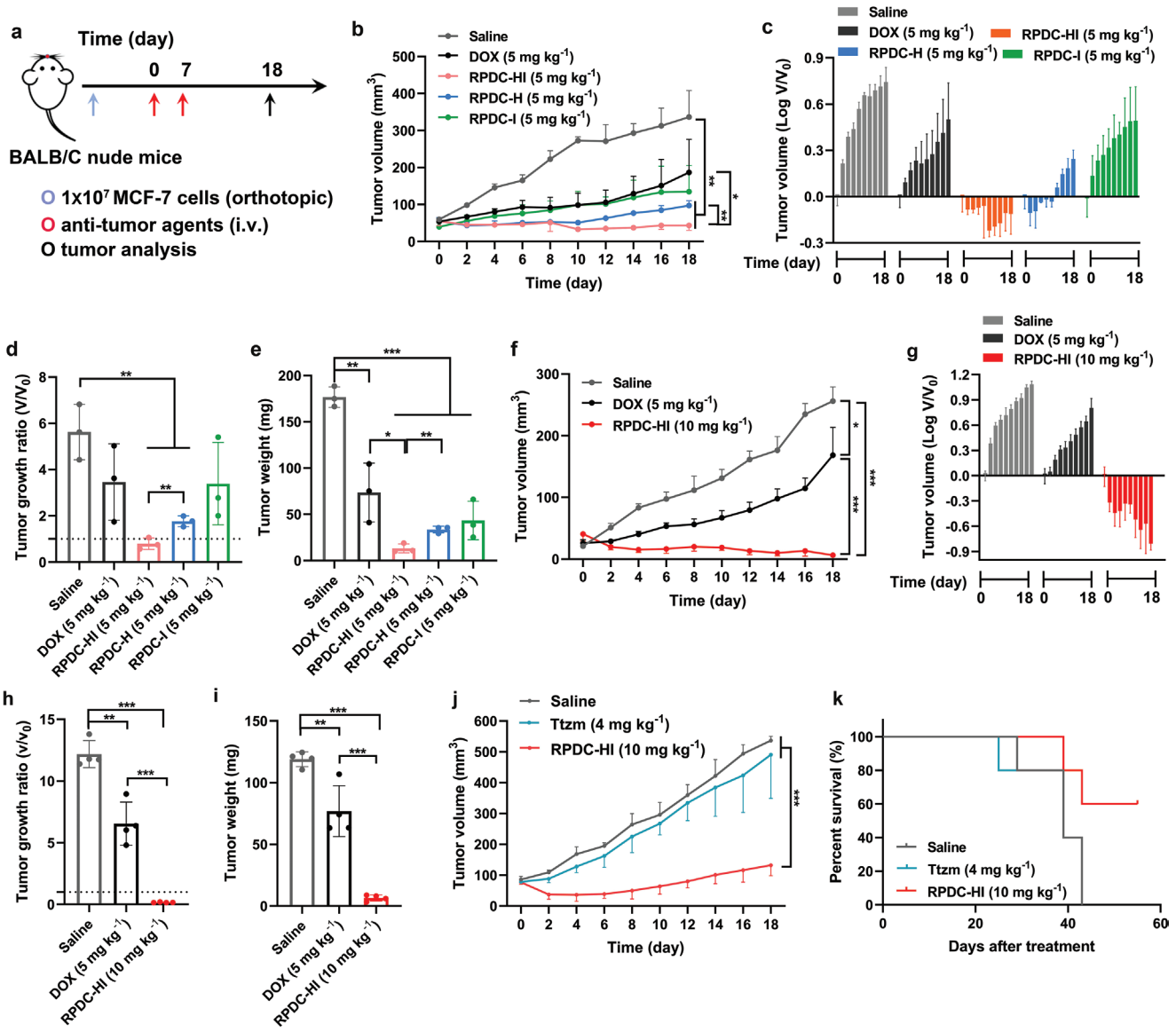

Figure 5. Antitumor efficiency of RPDC-HI. a) Timeline of tumor inoculation and treatment protocol. b–e) The changes of tumor volumes in the mice treated with 5 mg kg^{-1} free DOX and RPDCs (DOX eq.) from day 0 to day 18 (b,c). The tumor growth ratios (d) and tumor weights (e) in the mice treated with different agents measured at day 18, ($n = 3$). f–i) The changes of tumor volumes in the mice treated with 5 mg kg^{-1} free DOX and 10 mg kg^{-1} RPDC-HI (DOX eq.) from day 0 to day 18 (f,g). The tumor growth ratios (h) and tumor weights (i) in the mice treated with 5 mg kg^{-1} free DOX and 10 mg kg^{-1} RPDC-HI measured at day 18, ($n = 4$). j) The changes of tumor volumes in the mice treated with 4 mg kg^{-1} Ttzm and 10 mg kg^{-1} RPDC-HI (DOX eq.) from day 0 to day 18 ($n = 5$). k) Kaplan–Meier analysis of the mice treated with Ttzm and RPDC-HI. Data are presented as mean ± SD, statistical significances were calculated using unpaired *t*-test, $*p < 0.05$, $**p < 0.01$, $***p < 0.001$.

were 85, 29, and 0.6, respectively (Figure 6c and Table S1, Supporting Information). The average lung metastatic lesions of three groups treated with saline, free DOX, and RPDC-HI were 23, 32.2, and 1.3, respectively (Figure 6c and Table S1, Supporting Information). Meanwhile, we found that splenomegaly was induced in the mice with metastatic tumors, while it was significantly alleviated in RPDC-HI-treated group to approaching that of the healthy mice (Figure 6b). The average weights of the spleens for mice treated with saline, free DOX, and RPDC-HI were 545.5, 609.5, and 252.6 mg, respectively (Figure 6d and Table S1, Supporting Information), which were 2.5, 2.8, and 1.2 times higher than that of the healthy mice (213.9 mg). Splenic infiltration was observed in the saline group and free DOX group but not in the RPDC-HI group, suggesting that HER2 and integrin $\alpha_v\beta_3$ dual-targeted RPDC-HI protected the mice from metastatic cancer cells. H&E analysis of the collected tissue samples confirmed these observations (Figure 6e–g).

2.7. Downregulation of the Tumor Growth Signaling Pathways by Dual-Targeted RP-HI

Since the improved antitumor efficacy of RPDC-HI is possibly associated with synergistic actions of dual targeting of

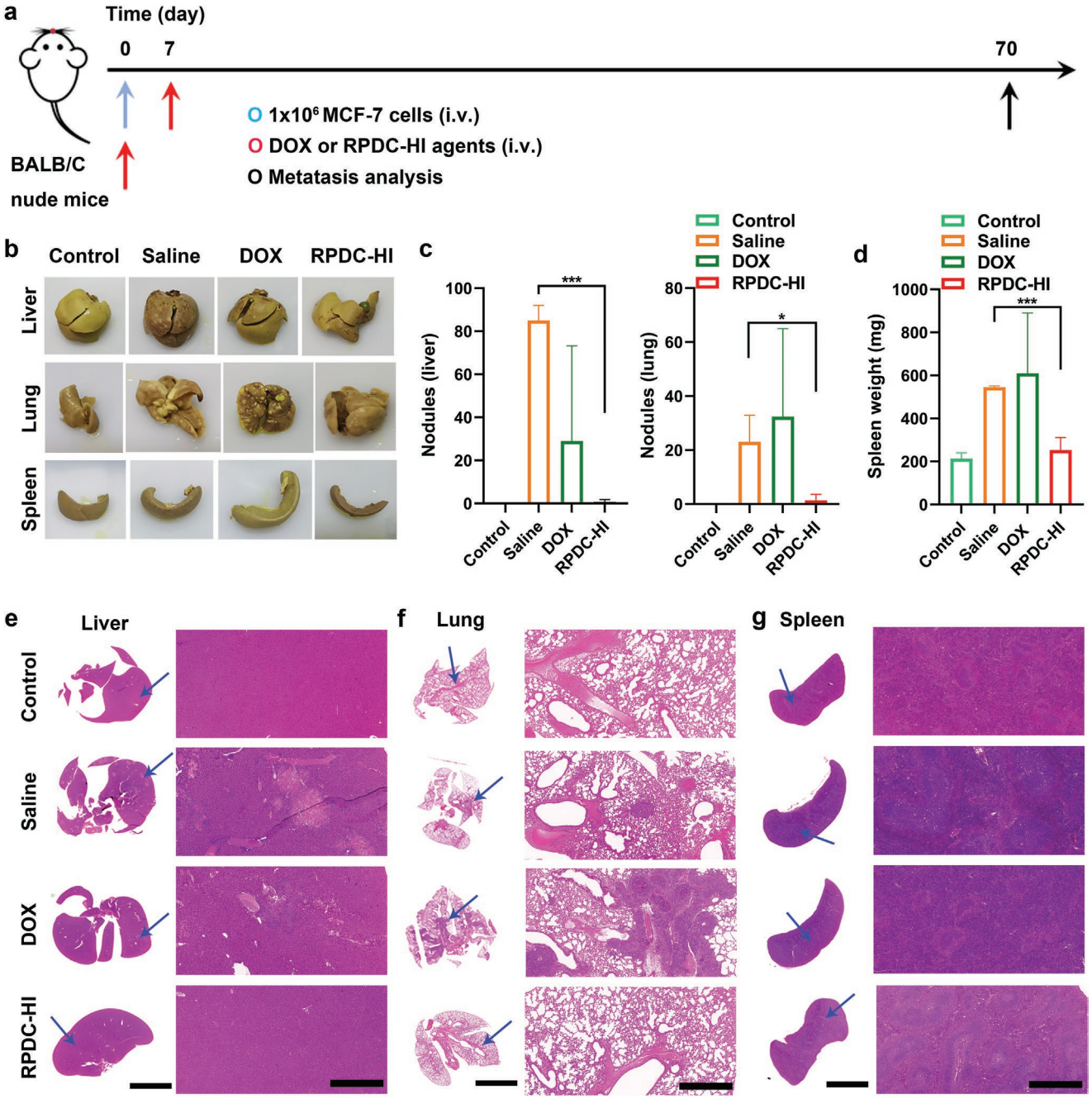

Figure 6. Inhibition of metastasis by dual-targeted RPDC-HI. a) Timeline of tumor metastasis model establishment and treatment protocol. b) Images of the livers, lungs, and spleens collected from mice treated with saline, DOX, and RPDC-HI, fixed with Bouin's solution. The organs from healthy mice were used as negative control. c) Tumor nodules in livers and lungs collected from the mice treated with different agents. d) Weights of spleen in the mice treated with different agents. e–g) H&E analysis of the liver (e), lung (f), and spleen (g) collected from the mice treated with saline, DOX, and RPDC-HI. The images of the whole tissue are shown on the left and one random region (where the arrows indicate) was selected, enlarged, and shown on the right. Scale bar = 6 mm (left), 800 µm (right) ($n = 3$ for Control, DOX and RPDC-HI groups; $n = 2$ for saline group). Data are presented as mean ± SD; statistical significances were calculated using multiple *t*-tests, $^{*}p < 0.05$, $^{***}p < 0.001$.

HER2 and integrin $\alpha_v\beta_3$ by RP-HI in disrupting tumor growth signal pathways, we evaluated downstream signaling pathways of the selected members of the HER family in MCF-7 cells after treatment. qRT-PCR analysis for quantifying the mRNA expression level and western immunoblot (WB) analysis for the protein expression level revealed that the significant blockade of HER family and reduced expression of integrin $\alpha_v\beta_3$ were achieved in MCF-7 cells treated with dual-targeted RP-HI after 24 h incubation (**Figure 7**a–c). The mRNA levels of *ERBB1, ERBB2, ERBB3,* and *ERBB4* in RP-HI-treated MCF-7 cells were down-regulated by 20%, 33%, 32%, and 17%, respectively, compared to those of PBS-treated control (Figure 7a). RP-HI treatment

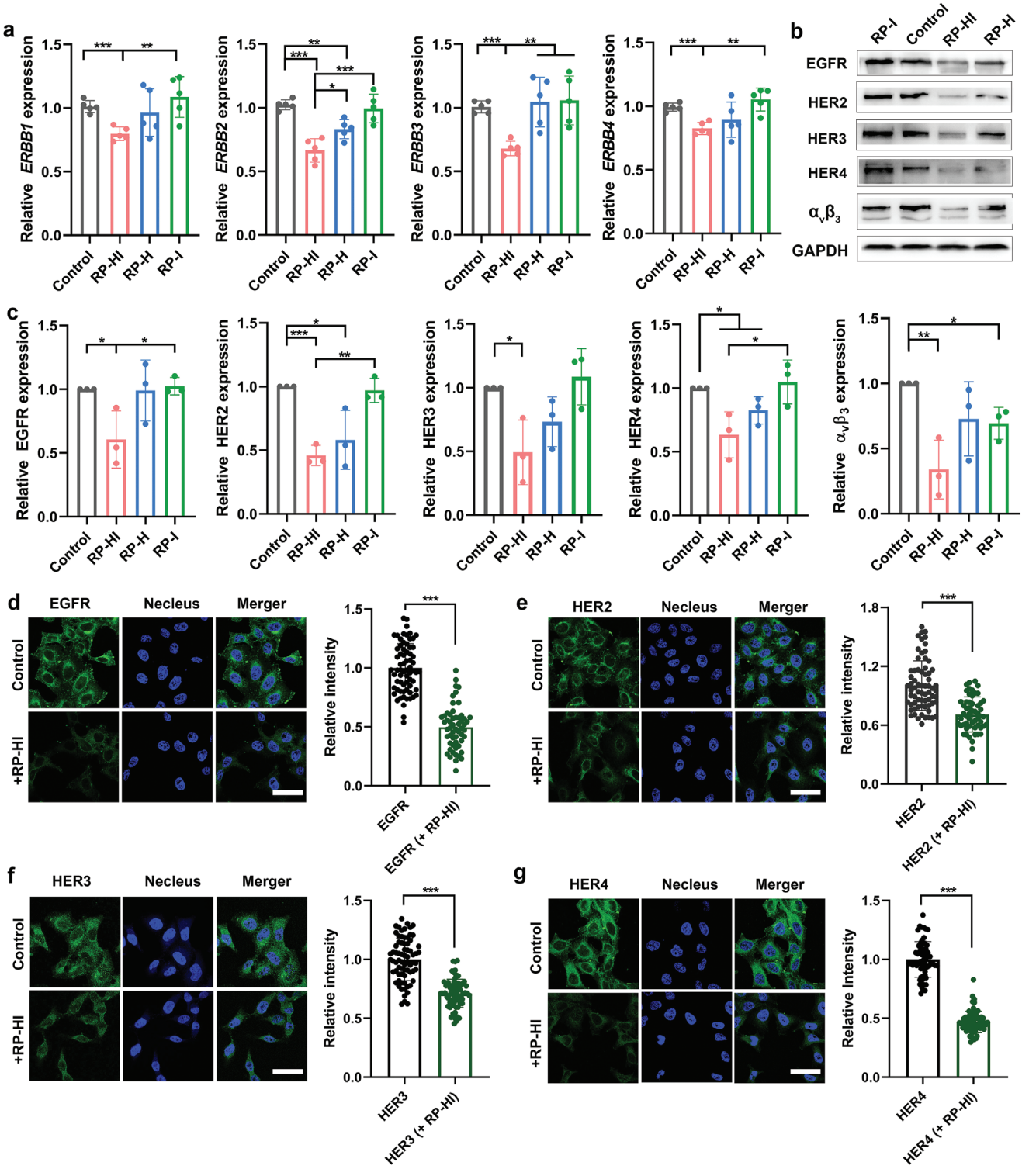

Figure 7. Downregulation of the tumor growth signaling pathways by dual-targeted RP-HI. a) The mRNA levels of *ERBB1*, *ERBB2*, *ERBB3*, and *ERBB4* in MCF-7 cells after treated with different RPs for 24 h ($n = 5$). b) WB analysis of the expressions of HER family members and integrin $\alpha_v\beta_3$ in MCF-7 cells after treated with different RPs for 24 h. c) Cumulative densitometric analyses of the WB images in (b) performed by ImageJ ($n = 3$). d–g) CLSM images of the expressions of EGFR (d), HER2 (e), HER3 (f), and HER4 (g) in RP-HI-treated MCF-7 cells measured by immunofluorescence ($n = 56$–72); scale bar = 50 µm. Data are presented as mean ± SD, statistical significances were calculated using unpaired *t*-test, $^*p < 0.05$, $^{**}p < 0.01$, $^{***}p < 0.001$.

also led to downregulation of the expression of EGFR, HER2, HER3, HER4, and integrin $\alpha_v\beta_3$ by 39%, 54%, 51%, 37%, and 66%, respectively, (Figure 7b,c) with extraordinarily significant downregulation of HER2, HER3, and integrin $\alpha_v\beta_3$. However, for RP-H and RP-I, they only downregulated the expression of HER2 or integrin that was directly targeted, and had little effects

on the expression of other members of HER family. The downregulation of EGFR, HER2, HER3, and HER4 in RP-HI-treated MCF-7 cells was further confirmed by immunofluorescence. The downregulation of the expression of EGFR, HER2, HER3, and HER4 was by 50%, 30%, 29%, and 53%, respectively, compared to that of control (Figure 7d–g). Importantly, RP-HI was able to inhibit the activation of PI3K, AKT, and steroid receptor co-activator (SRC) that involved in the downstream signaling pathways (Figure S15, Supporting Information). In contrast, HER2 single-targeted RP-H could not downregulate either the total expression or the phosphorylation of PI3K, AKT, and SRC (P-PI3K, P-AKT, and P-SRC). Similarly, integrin single targeted RP-I showed a negligible effect on the expression and phosphorylation of downstream signal molecules. Taking together, these results support that simultaneously blocking HER2 and integrin $\alpha_v\beta_3$ with RP-HI can effectively downregulate the expression of all members of HER family and further inhibit several specific downstream signaling pathways.

3. Discussion and Conclusion

HER2 has been long considered as an effective and successful drug target, supported by the clinical evidence of improved survival of HER2-positive breast cancer patients.[25] However, increasing findings shows that blocking HER2 alone is not enough to inhibit the abnormal tumor growth signals,[9a] as majority of tumors that initially respond to HER2-targeted antibody treatment with Ttzm recur within 1 year.[26] The drug resistance and tumor recurrence after HER2-targeted therapy has become a significant clinical challenge when managing HER2-positive patients. First, latest studies indicate that there are compensation mechanisms provided by overexpression or amplification of other members in the HER family, including EGFR[27] and HER3,[28] to enable cancer escaping or coping with HER2 targeted treatment. Thus, the strategy of targeting multiple HERs has been proposed. Preclinical evidence suggests that co-inhibition of HER2 and other HERs by combination therapy might prevent or prolong time to resistance and treatment failure.[29] Second, in addition to compensation mechanism which causes treatment failure, HER family-targeting therapy also can upregulate the expression of integrin in cancer cells,[23] and causes the integrin-mediated signaling activation, such as PI3K/AKT.[16] Third, heterogeneous HER2 amplification in primary and metastatic tumor has become a great barrier for achieving good benefit from treatment of HER2-specfic monoclonal antibodies and ADCs.[12a,25] To address these issues that we face in breast cancer treatment, we design the reported HER2 and integrin $\alpha_v\beta_3$ dual-targeted RP-HI and RPDC-HI. With simultaneously targeting HER2 and integrin $\alpha_v\beta_3$, RP-HI exhibited a great ability to reduce the expressions of the HER family and integrins, including EGFR, HER2, HER3, and HER4 at both mRNA and protein levels and $\alpha_v\beta_3$ at protein level, leading to a significant inhibition of the downstream signaling pathways including PI3K/AKT and SRC, a common event downstream of various signaling pathways in Ttzm resistance.[30] More importantly, the HER2 and integrin $\alpha_v\beta_3$ dual-targeted RPDC-HI can significantly reduce tumor volume rather than inhibiting tumor growth only. Moreover, the antimetastasis activity of RPDC-HI is much high.

In addition to providing signaling blockade by delivered antibodies and ligands, the reported RPDCs demonstrated several advantages in combined delivery of different agents using a single biomolecular platform. We used nanobody, ligand, and recombinant protein as the substitute of conventional antibodies to design an HER2 and integrin $\alpha_v\beta_3$ dual-targeted RPDC-HI, which could achieve a specific drug delivery to the tumor sites and minimized the drug distribution in normal organs, leading to the superior antitumor and antimetastasis efficiency for HER2-positive MCF-7 tumors. This molecule platform of RPDC-HI provides several benefits for breast cancer therapy: 1) inhibiting whole HER family and blocking downstream signaling pathways through HER2 and integrin $\alpha_v\beta_3$ dual targeting design; 2) acid-labile linker offering tumor-specific drug release; and 3) optimized tumoral accumulation and diffusion, resulting a homogeneous drug distribution in tumor mass and significant tumor volume reduction as well as great antimetastasis efficiency. Poor penetration ability for solid tumors is the challenge for traditional ADCs. Moreover, the nonspecificity for tissues and short circulation time limited the applications of the rising peptide–drug conjugates (PDCs). Comparing to ADCs and PDCs, RPDCs we developed have advantages including high specificity due to its dual-targeted structure and good penetration ability since its size is much smaller than the conventional ADCs. Therefore, RPDCs have great clinical translation potentials.

Supporting Information

Supporting Information is available from the Wiley Online Library or from the author.

Acknowledgements

This study was supported by the National Key R&D Program of China (Nos. 2017YFA0701301 and 2017YFA0205400), the Natural Science Foundation of China (Nos. 92163214, 51690153, 21720102005, and 51803089) and the Natural Science Foundation of Jiangsu Province (BK20202002). All animal experiments were performed in compliance with guidelines set by the Animal Ethical and Welfare Committee at Nanjing University (Nanjing, China) (ID: 2003100).

Conflict of Interest

Y.Y., W.C. and X.J. have a patent application related to this work.

Data Availability Statement

The data that support the findings of this study are available from the corresponding author upon reasonable request.

Keywords

drug delivery, epidermal growth factor receptor family, epidermal growth factor receptor type 2, integrins, recombinant proteins

Received: February 16, 2022
Revised: March 30, 2022
Published online: May 4, 2022

[1] N. Harbeck, F. Penault-Llorca, J. Cortes, M. Gnant, N. Houssami, P. Poortmans, K. Ruddy, J. Tsang, F. Cardoso, *Nat. Rev. Dis. Primers* **2019**, *5*, 66.
[2] a) F. Meric-Bernstam, A. M. Johnson, E. Dumbrava, K. Raghav, S. A. Piha-Paul, *Clin. Cancer Res.* **2019**, *25*, 2033; b) J. Nico, S. Rita, H. Elisabeth, E. Andreas, *Cancers* **2017**, *9*, 33.
[3] D. J. Slamon, G. M. Clark, S. G. Wong, W. J. Levin, A. Ullrich, W. L. McGuire, *Science* **1987**, *235*, 177.
[4] C. E. Geyer, J. Forster, D. Lindquist, S. Chan, C. G. Romieu, T. Pienkowski, A. Jagiello-Gruszfeld, J. Crown, A. Chan, B. Kaufman, D. Skarlos, M. Campone, N. Davidson, M. Berger, C. Oliva, S. D. Rubin, S. Stein, D. Cameron, *N. Engl. J. Med.* **2006**, *355*, 2733.
[5] W. Scheuer, T. Friess, H. Burtscher, B. Bossenmaier, J. Endl, M. Hasmann, *Cancer Res.* **2009**, *69*, 9330.
[6] J. M. Lambert, R. V. Chari, *J. Med. Chem.* **2014**, *57*, 6949.
[7] a) B. N. Rexer, C. L. Arteaga, *Crit. Rev. Oncog.* **2012**, *17*, 1; b) L. Gianni, U. Dafni, R. D. Gelber, E. Azambuja, S. Muehlbauer, A. Goldhirsch, M. Untch, I. Smith, J. Baselga, C. Jackisch, D. Cameron, M. Mano, J. L. Pedrini, A. Veronesi, C. Mendiola, A. Pluzanska, V. Semiglazov, E. Vrdoljak, M. J. Eckart, Z. Shen, G. Skiadopoulos, M. Procter, K. I. Pritchard, M. J. Piccart-Gebhart, R. Bell, *Lancet Oncol.* **2011**, *12*, 236.
[8] C. L. Vogel, M. A. Cobleigh, D. Tripathy, J. C. Gutheil, L. N. Harris, L. Fehrenbacher, D. J. Slamon, M. Murphy, W. F. Novotny, M. Burchmore, S. Shak, S. J. Stewart, M. Press, *J. Clin Oncol.* **2002**, *20*, 719.
[9] a) Y. Yarden, M. X. Sliwkowski, *Nat. Rev. Mol. Cell Biol.* **2001**, *2*, 127; b) C. A. Ritter, M. Perez-Torres, C. Rinehart, M. Guix, T. Dugger, J. A. Engelman, C. L. Arteaga, *Clin. Cancer Res.* **2007**, *13*, 4909.
[10] J. T. Garrett, M. G. Olivares, C. Rinehart, N. D. Granja-Ingram, V. Sanchez, A. Chakrabarty, B. Dave, R. S. Cook, W. Pao, E. McKinely, H. C. Manning, J. Chang, C. L. Arteaga, *Proc. Natl. Acad. Sci. USA* **2011**, *108*, 5021.
[11] a) D. Graus-Porta, R. R. Beerli, J. M. Daly, N. E. Hynes, *EMBO J.* **1997**, *16*, 1647; b) T. Holbro, R. R. Beerli, F. Maurer, M. Koziczak, C. Barbas, N. E. Hynes, *Proc. Natl. Acad. Sci. U. S. A.* **2003**, *100*, 8933; c) N. V. Sergina, M. Rausch, D. Wang, J. Blair, B. Hann, K. M. Shokat, M. M. Moasser, *Nature* **2007**, *445*, 437.
[12] a) O. M. Filho, G. Viale, S. Stein, L. Trippa, D. A. Yardley, I. A. Mayer, V. G. Abramson, C. L. Arteaga, L. M. Spring, A. G. Waks, E. Wrabel, M. K. DeMeo, A. Bardia, P. Dell'Orto, L. Russo, T. A. King, K. Polyak, F. Michor, E. P. Winer, I. E. Krop, *Cancer Discovery* **2021**, *11*, 2474; b) C. M. Yamazaki, A. Yamaguchi, Y. Anami, W. Xiong, Y. Otani, J. Lee, N. T. Ueno, N. Zhang, Z. An, K. Tsuchikama, *Nat. Commun.* **2021**, *12*, 3528.
[13] a) D. A. Ferraro, N. Gaborit, R. Maron, H. Cohen-Dvashi, Z. Porat, F. Pareja, S. Lavi, M. Lindzen, N. Ben-Chetrit, M. Sela, Y. Yarden, *Proc. Natl. Acad. Sci. U. S. A.* **2013**, *110*, 1815; b) J. J. Tao, P. Castel, N. Radosevic-Robin, M. Elkabets, N. Auricchio, N. Aceto, G. Weitsman, P. Barber, B. Vojnovic, H. Ellis, N. Morse, N. T. Viola-Villegas, A. Bosch, D. Juric, S. Hazra, S. Singh, P. Kim, A. Bergamaschi, S. Maheswaran, T. Ng, F. Penault-Llorca, J. S. Lewis, L. A. Carey, C. M. Perou, J. Baselga, M. Scaltriti, *Sci. Signaling* **2014**, *7*, ra29.
[14] E. Tzahar, H. Waterman, X. Chen, G. Levkowitz, D. Karunagaran, S. Lavi, B. J. Ratzkin, Y. Yarden, *Mol. Cell. Biol.* **1996**, *16*, 5276.
[15] E. C. da Silva, M. Dontenwill, L. Choulier, M. Lehmann, *Cancers* **2019**, *11*, 692.
[16] A. B. Hanker, M. V. Estrada, G. Bianchini, P. D. Moore, J. Zhao, F. Cheng, J. P. Koch, L. Gianni, D. R. Tyson, V. Sanchez, B. N. Rexer, M. E. Sanders, Z. Zhao, T. P. Stricker, C. L. Arteaga, *Cancer Res.* **2017**, *77*, 3280.
[17] a) H. Hamidi, J. Ivaska, *Nat. Rev. Cancer* **2018**, *18*, 533; b) K. L. Harper, M. S. Sosa, D. Entenberg, H. Hosseini, J. F. Cheung, R. Nobre, A. Avivar-Valderas, C. Nagi, N. Girnius, R. J. Davis, E. F. Farias, J. Condeelis, C. A. Klein, J. A. Aguirre-Ghiso, *Nature* **2016**, *540*, 588.
[18] a) J. M. Ricono, M. Huang, L. A. Barnes, S. K. Lau, S. M. Weis, D. D. Schlaepfer, S. K. Hanks, D. A. Cheresh, *Cancer Res.* **2009**, *69*, 1383; b) W. Guo, Y. Pylayeva, A. Pepe, T. Yoshioka, W. J. Muller, G. Inghirami, F. G. Giancotti, *Cell* **2006**, *126*, 489; c) C. Huang, C. C. Park, S. G. Hilsenbeck, R. Ward, M. F. Rimawi, Y.-c. Wang, J. Shou, M. J. Bissell, C. K. Osborne, R. Schiff, *Breast Cancer Res.* **2011**, *13*, R84.
[19] J. S. Desgrosellier, D. A. Cheresh, *Nat. Rev. Cancer* **2010**, *10*, 9.
[20] Y. Barenholz, *J. Controlled Release* **2012**, *160*, 117.
[21] C. J. Witton, J. R. Reeves, J. J. Going, T. G. Cooke, J. Bartlett, *J. Pathol.* **2003**, *200*, 290.
[22] J. Liu, Z. Zhao, N. Qiu, Q. Zhou, G. Wang, H. Jiang, Y. Piao, Z. Zhou, J. Tang, Y. Shen, *Nat. Commun.* **2021**, *12*, 2425.
[23] W. Chen, Y. Yuan, C. Li, H. Mao, B. Liu, X. Jiang, *Adv. Mater.* **2022**, *34*, 2109376.
[24] E. H. Romond, E. A. Perez, J. Bryant, V. J. Suman, C. E. Geyer, N. E. Davidson, E. Tan-Chiu, S. Martino, S. Paik, P. A. Kaufman, S. M. Swain, T. M. Pisansky, L. Fehrenbacher, L. A. Kutteh, V. G. Vogel, D. W. Visscher, G. Yothers, R. B. Jenkins, A. M. Brown, S. R. Dakhil, E. P. Mamounas, W. L. Lingle, P. M. Klein, J. N. Ingle, N. Wolmark, *N. Engl. J. Med.* **2005**, *353*, 1673.
[25] D. Y. Oh, Y. J. Bang, *Nat. Rev. Clin. Oncol.* **2020**, *17*, 33.
[26] R. Nahta, F. J. Esteva, *Cancer Lett.* **2006**, *232*, 123.
[27] K. C. Day, G. L. Hiles, M. Kozminsky, S. J. Dawsey, A. Paul, L. J. Broses, R. Shah, L. P. Kunja, C. Hall, N. Palanisamy, S. Daignault-Newton, L. El-Sawy, S. J. Wilson, A. Chou, K. W. Ignatoski, E. Keller, D. Thomas, S. Nagrath, T. Morgan, M. L. Day, *Cancer Res.* **2017**, *77*, 74.
[28] T. Holbro, R. R. Beerli, F. Maurer, M. Koziczak, C. F. Barbas, N. E. Hynes, *Proc. Natl. Acad. Sci. U. S. A.* **2003**, *100*, 8933.
[29] N. O'Donovan, A. T. Byrne, A. E. O'Connor, S. McGee, W. M. Gallagher, J. Crown, *Invest. New Drugs* **2011**, *29*, 752.
[30] S. Zhang, W.-C. Huang, P. Li, H. Guo, S.-B. Poh, S. W. Brady, Y. Xiong, L.-M. Tseng, S.-H. Li, Z. Ding, A. A. Sahin, F. J. Esteva, G. N. Hortobagyi, D. Yu, *Nat. Med.* **2011**, *17*, 461.